

# Constraining pulsar gap models with light-curve shapes and flux properties of a simulated $\gamma$ -ray pulsar population

Marco Pierbattista<sup>1</sup>, Isabelle A. Grenier<sup>1</sup>, Alice K. Harding<sup>2</sup>, Peter L. Gonthier<sup>3</sup>

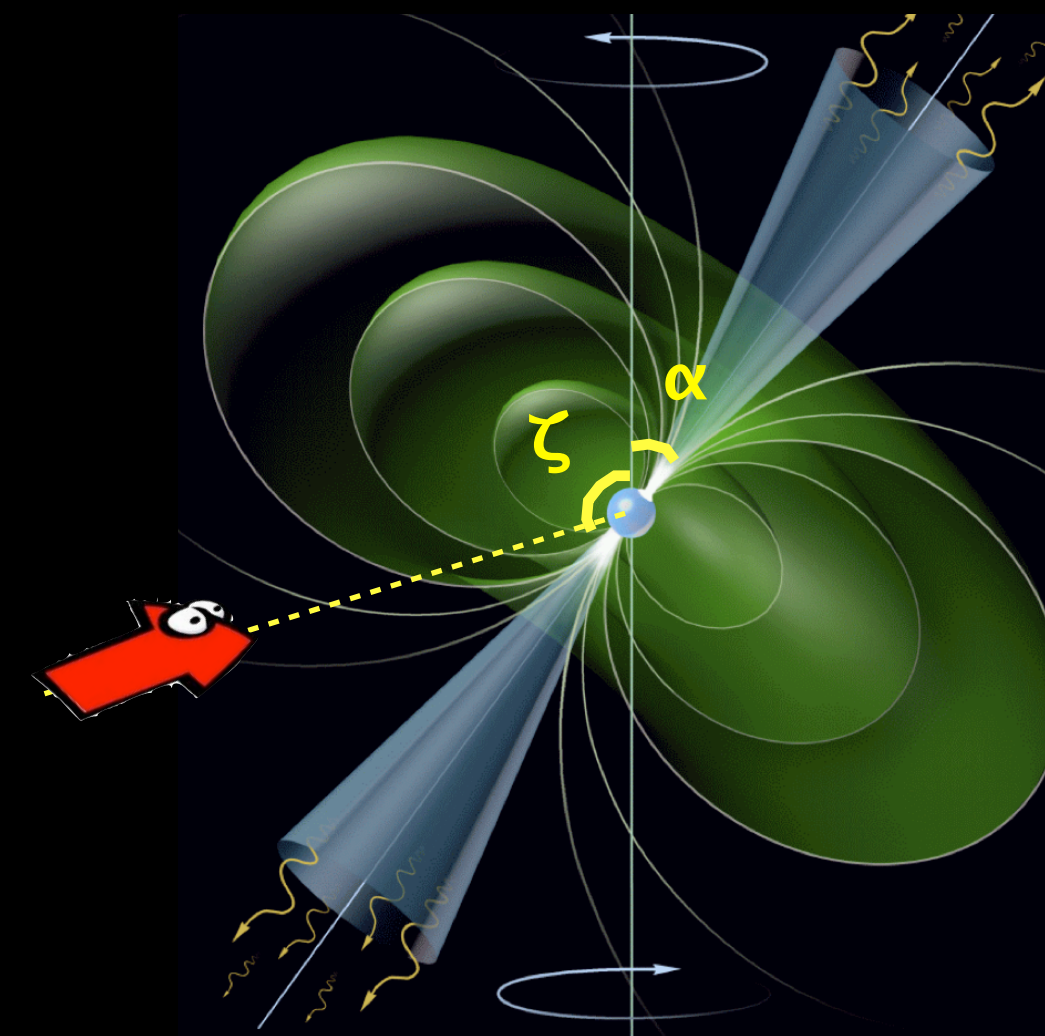
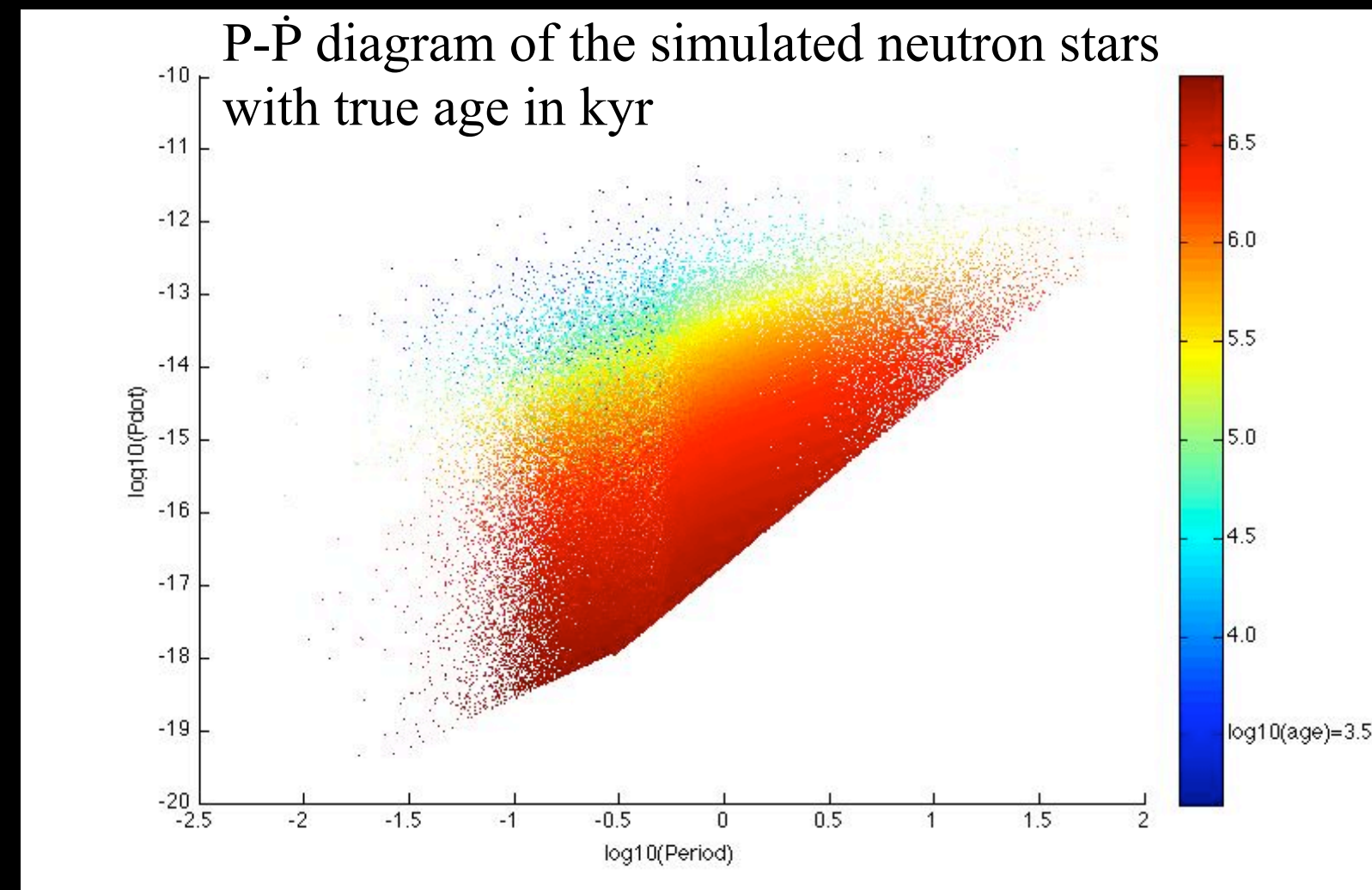
1- AIM, CEA-Irfu-Saclay & Université Paris Diderot 2- NASA Goddard Space Flight Center 3- Hope College, Department of Physics

## ABSTRACT

The Fermi Gamma-Ray Space Telescope has successfully discovered many  $\gamma$ -ray pulsars, both as radio-loud objects and radio-quiet or radio-weak pulsars that have been discovered through blind period searches. The latter presumably have  $\gamma$ -ray beams emanating at high altitudes in the magnetosphere, resulting in little or no overlap with the radio beam. The exponential cut-off of the emission at high energy also points to a medium- or high-altitude origin of the  $\gamma$  rays. Population synthesis offers the possibility to study two different statistical aspects of the  $\gamma$ -ray pulsar population: energetics and light curve geometry. The luminosity and efficiency behavior with respect to the main intrinsic parameters (age, magnetic field and gap width) offers a good way to constrain the pulsar energetics in the different models in competition (slot gap and outer gap). In parallel, the study of the light curve structures (peak multiplicity, position, and separation, and shape distributions) could provide a powerful method of constraining the pulsar beam geometry (position of magnetic and rotational axes respect to the line of sight, source altitude). New simulation results are compared below with Fermi pulsar data to probe the origin of the pulsed  $\gamma$  rays.

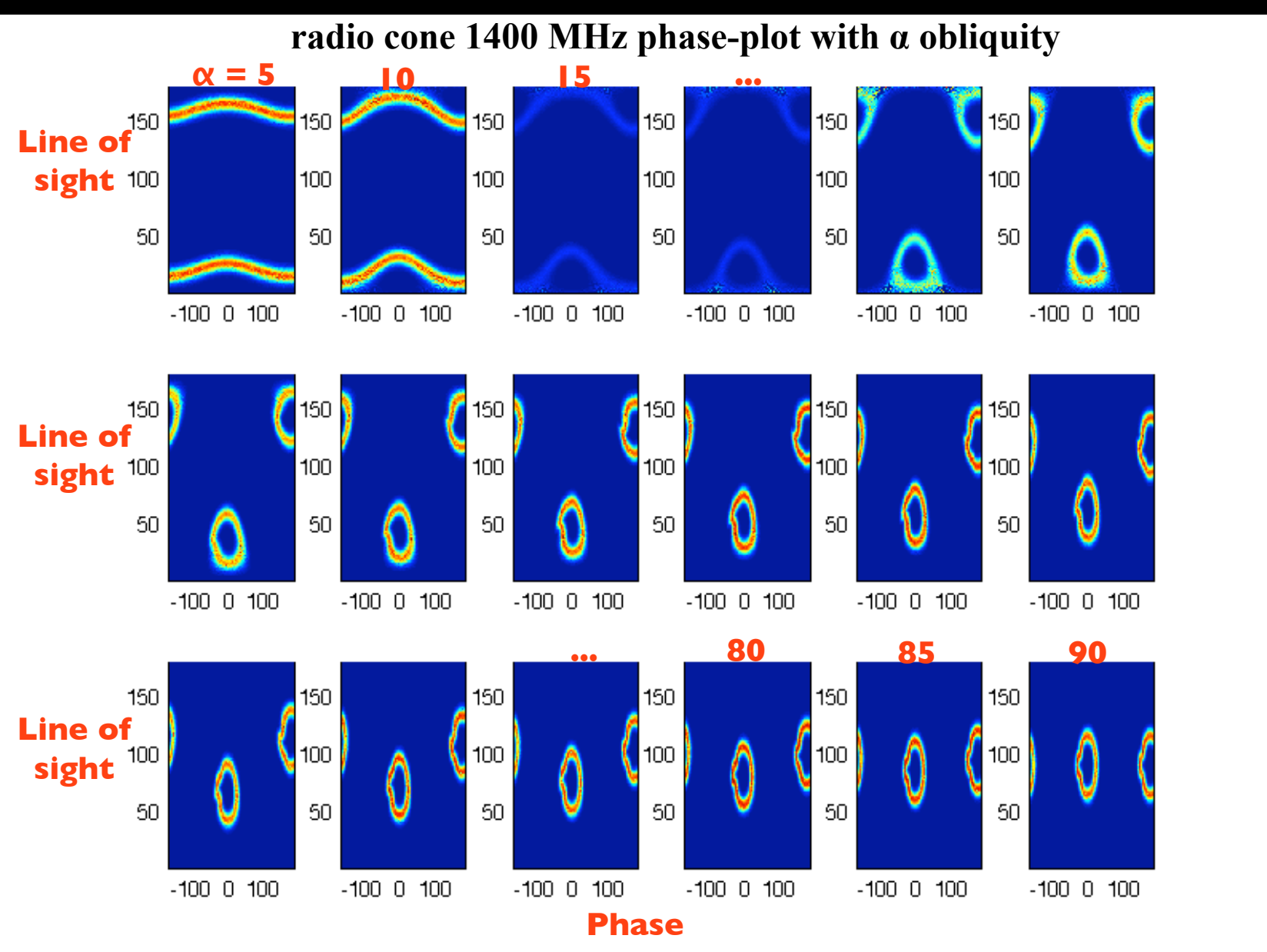
## ISOLATED NEUTRON STAR SAMPLE

We have evolved simulated neutron stars in the Galactic gravitational potential. Their birth properties (period  $P$ , its derivative  $\dot{P}$ , random spin & magnetic axes) and radio luminosity in the core and cone beams have been tuned to match the observed distributions in the ATNF catalogue (see poster P2-86, Gonthier et al.). A magnetic field decay timescale of 2.8 Myr has been used. The total number of simulated pulsars with radio flux larger than the sensitivity threshold of ten of the major radio pulsar surveys in the ATNF catalogue has been scaled to the actual number of detections in these surveys.



## PHASEPLOTS

To obtain realistic light curves, we have generated phase-plots that reproduce the distribution of photons in rotational phase across the sky. The calculation includes the magnetic field retardation, light travel delays and relativistic aberration. Phase plots were produced to sample the magnetic obliquities ( $\alpha$ ) and pulsar characteristics relevant to each radio and  $\gamma$ -ray beam model ( $P$ ,  $\dot{P}$ ,  $B$ , gap width).



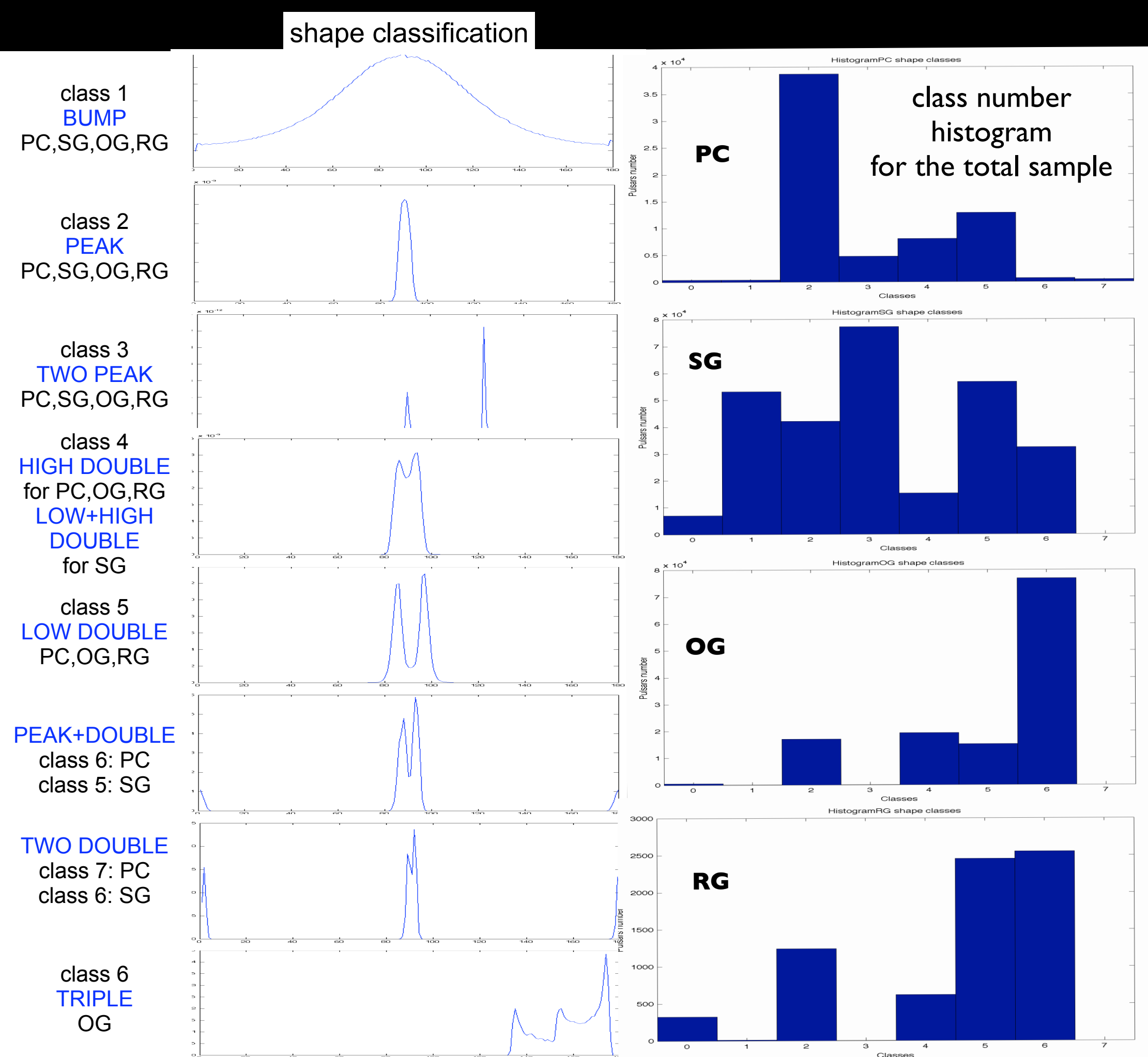
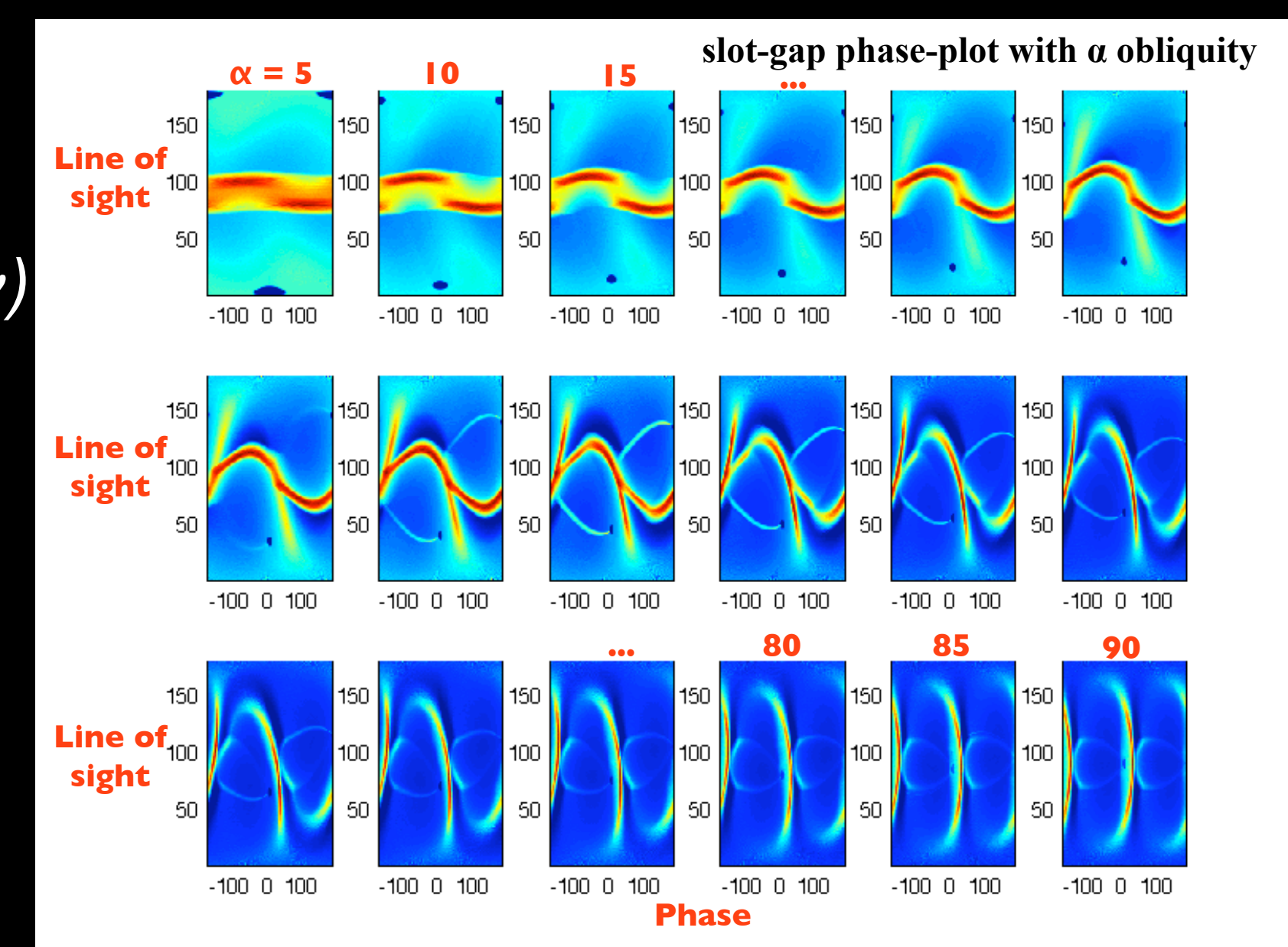
## LUMINOSITY MODELS

Radio luminosities were computed at  $\nu = 400$  and 1400 MHz for the core and cone components of the emission, for a total luminosity of  $L_{tot} = 6.98 \times 10^9 P^{-1} \dot{P}^{0.35} [mJy kpc^2 MHz]$  and core-to-cone peak flux ratio  $r = f(P, \nu)$

We implemented 4  $\gamma$ -ray models: the low-altitude slot gap (PC)<sup>(1)</sup>, the high-altitude slot gap (SG)<sup>(2)</sup>, the outer gap (OG)<sup>(3) & (4)</sup>, a variation of the outer gap (RG)<sup>(5)</sup>.

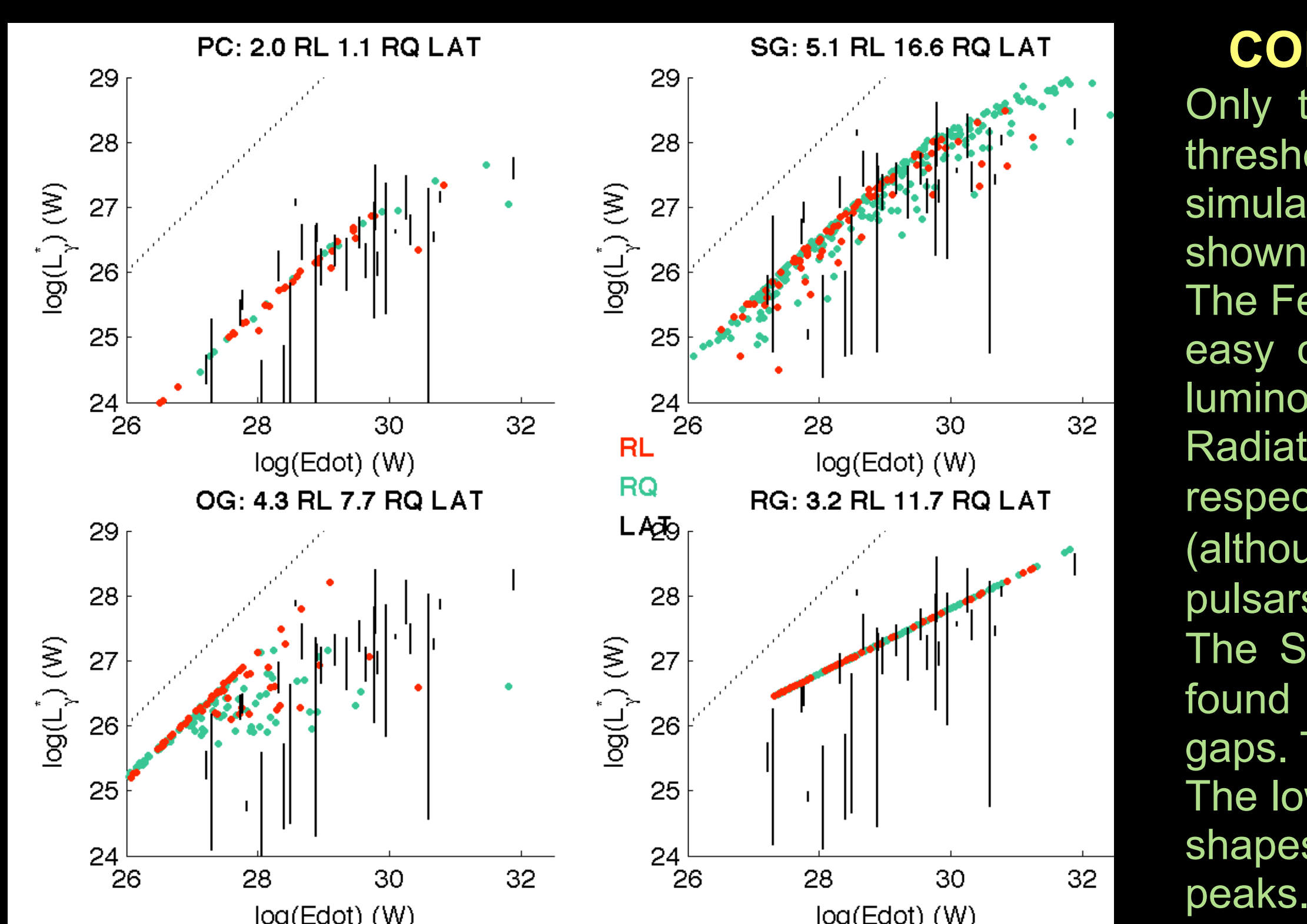
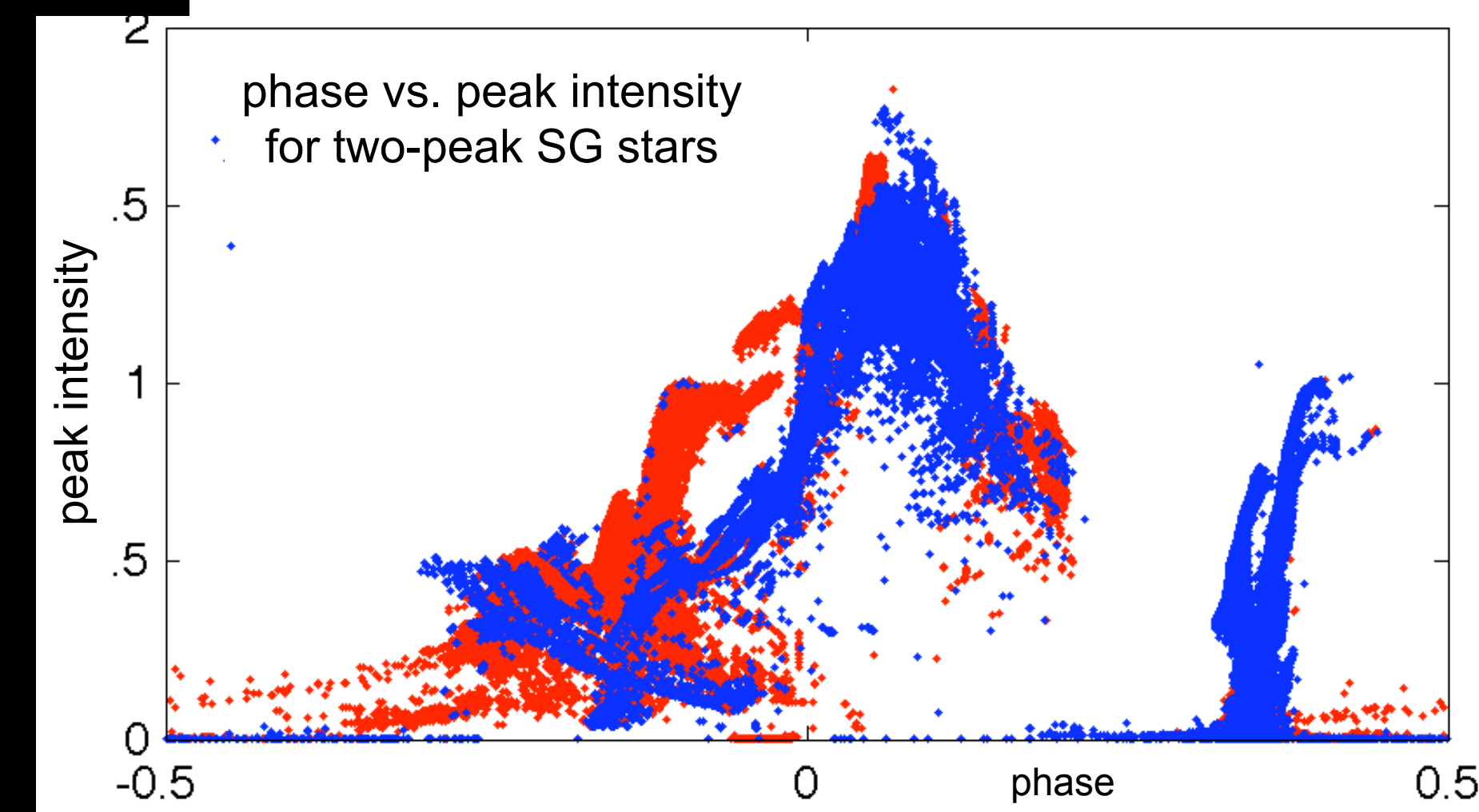
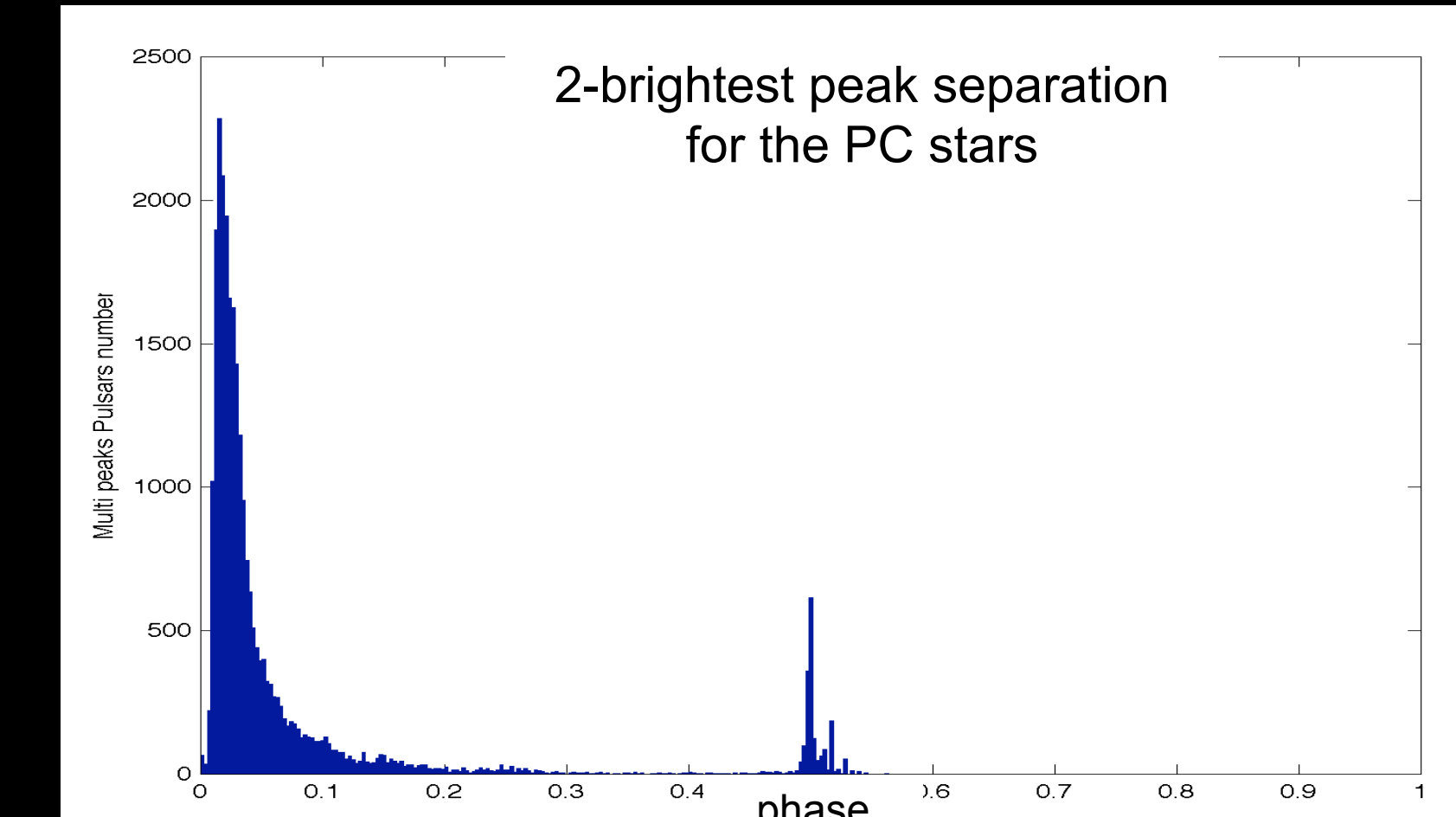
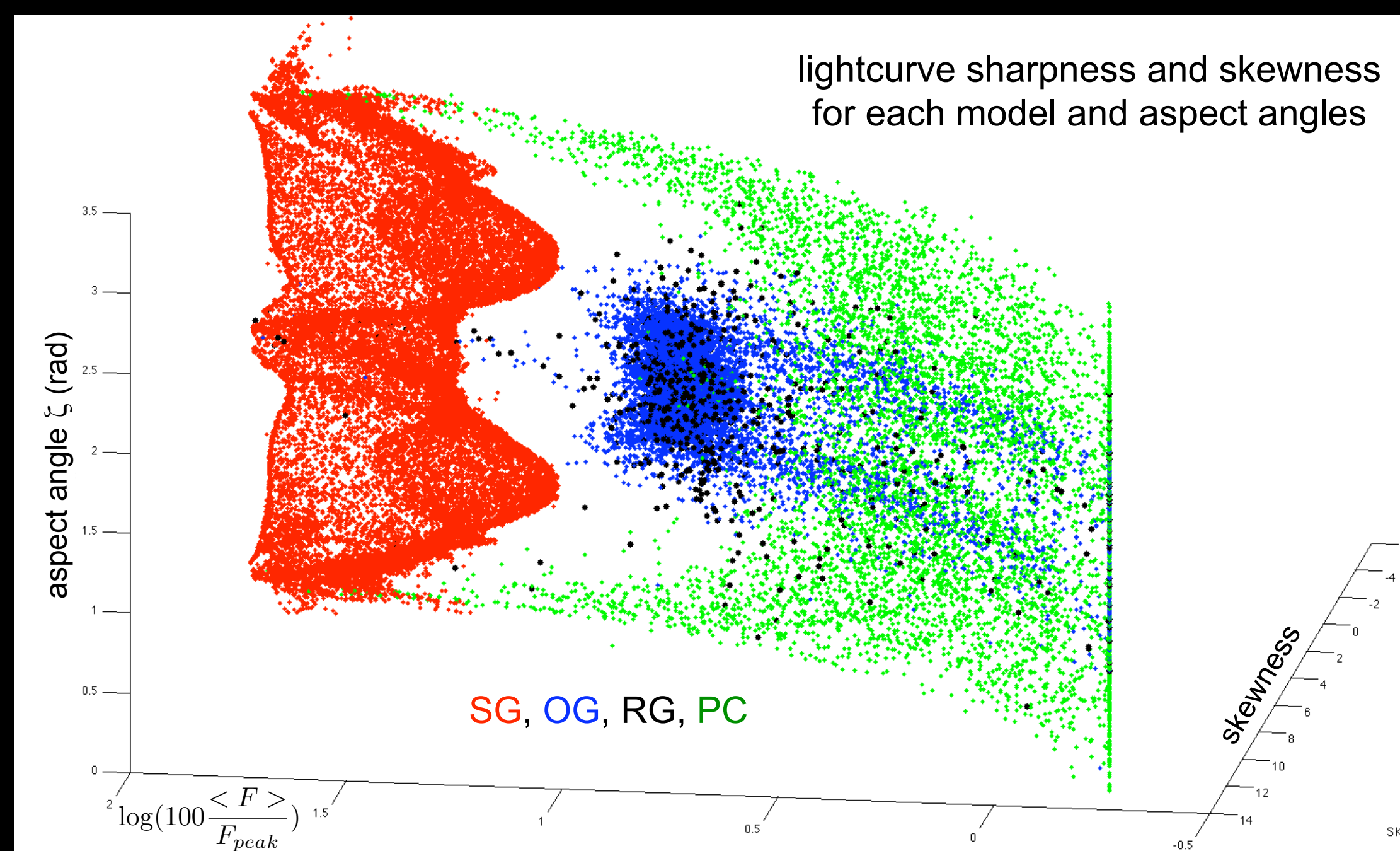
$$PC \ \& \ SG: L_\gamma \propto \epsilon_\gamma \dot{E} \Delta \xi^3 \quad OG: L_\gamma \propto \epsilon_\gamma \dot{E} \Delta w^3 \quad RG: L_\gamma \propto \epsilon_\gamma \dot{E} \Delta w$$

with radiative efficiencies,  $\epsilon_\gamma$ , and gap widths,  $\Delta \xi$  and  $\Delta w$ , depending on  $P$  and  $\dot{P}$ . The resulting fluxes above 100 MeV have been compared to the 6-month sensitivity threshold for the Fermi LAT observations to allow comparison with the Fermi pulsars<sup>(6)</sup>,



## PROPERTIES OF THE SIMULATED LIGHT CURVE SHAPES

Examples of light curve characteristics and statistics. Light curves have been grouped into classes characterized by their peak number and contrast. In these figures we plot all the pulsars of each model, without any visibility filter.



## COMPARISON OF THE SIMULATED AND REAL FERMI PULSARS

Only the simulated stars with a  $\gamma$ -ray flux,  $S_\gamma$ , higher than the Fermi sensitivity threshold have been retained in the following plots. A sample of properties for the simulated radio-loud (red), radio-quiet (green), and real Fermi (black) samples are shown for the four models.

The Fermi latitude histograms have been scaled to the total simulated visible counts to easy comparison. The latitude distributions of the 4 models reflect the underlying luminosity distributions, with younger, brighter, objects lying closer to the plane. Radiative efficiencies of 30, 100, 50, and 20 % for the PC, SG, OG, and RG, respectively, yield  $\gamma$ -ray luminosities in reasonable agreement with the observations (although too high for the outer gaps). Yet, the total number of visible simulated  $\gamma$ -ray pulsars is 2 to 3 times lower than the 38 young isolated pulsars seen by Fermi. The  $S_\gamma D^2$  brightness evolution with characteristic age (all observable variables) is found in reasonable agreement with the data for the slot gaps, less so for the outer gaps. The spread in the Fermi data is, however, not discriminating. The low-altitude model is unfavoured on spectral grounds, as well as in the light curve shapes. The standard outer gap lacks bright young objects with widely separated peaks.

